International Journal of Pharmaceutics: X 8 (2024) 100280

Contents lists available at ScienceDirect

International Journal of Pharmaceutics: X

journal homepage: www.sciencedirect.com/journal/international-journal-of-pharmaceutics-x

Resveratrol liposomes reverse sorafenib resistance in renal cell carcinoma models by modulating PI3K-AKT-mTOR and VHL-HIF signaling pathways

Ligang Wang [a,1], Ying Wang [b,1], Qiqi Xie [c,1], Songcheng Xu [a], Chen Yang [a], Fei Liu [d], Yang Liu [a], Fuwei Wang [e], Weinan Chen [a,*], Jianchun Li [a,*], Litao Sun [a,*]

[a] *Cancer Center, Department of Ultrasound Medicine, Zhejiang Provincial People's Hospital, Affiliated People's Hospital, Hangzhou Medical College, Hangzhou, Zhejiang, China*

[b] *Health Management Center, Health Promotion Center, Zhejiang Provincial People's Hospital, Affiliated People's Hospital, Hangzhou Medical College, Hangzhou, Zhejiang, China*

[c] *Heart Center, Department of Cardiovascular Medicine, Zhejiang Provincial People's Hospital, Affiliated People's Hospital, Hangzhou Medical College, Hangzhou, Zhejiang, China*

[d] *Center for Rehabilitation Medicine, Rehabilitation & Sports Medicine Research Institute of Zhejiang Province, Department of Rehabilitation Medicine, Zhejiang Provincial People's Hospital (Affiliated People's Hospital), Hangzhou Medical College, Hangzhou, Zhejiang, China.*

[e] *Department of Oncology and Cancer Biotherapy Center, Zhejiang Provincial People's Hospital, Hangzhou, Zhejiang 310014, China*

A R T I C L E I N F O

Keywords:
Resveratrol liposomes
Sorafenib
Resistance
Combination
Renal cell carcinoma
PI3K-AKT-mTOR
VHL-HIF
Signaling pathway

A B S T R A C T

RCC is a malignant tumor arising from the urothelium of renal parenchyma that remains challenging to be treated. In this study, we assessed the anti-tumor effects of Resveratrol liposomes (RES-lips) combined with sorafenib on renal cell carcinoma (RCC) and explored the potential mechanisms underlying the improvement of sorafenib resistance models. Tumor growth and survival following treatment with sorafenib alone or in combination with RES-lips was evaluated in a RCC xenograft mouse model. Flow cytometry results demonstrated that the combination of RES-lips and sorafenib significantly enhanced the G1/S phase arrest of sorafenib-resistant cells. When compared with the PBS or monotherapy groups, treatment with RES-lips combined with sorafenib exhibited significant inhibition of tumor growth in the RCC xenograft mouse model with tumor growth inhibition (TGI) rates and complete remission (CR) rates of 90.1 % and 50 %, respectively. Concersely, the maximum TGI rate was 53.6 % in the RES-lips monoherapy group and 29.2 % and in the sorafenib monotherapy group, and no animals achieved CR. Additionally, the current combination therapy promoted the proliferation of unactivated splenic lymphocytes and the proliferation of soybean protein A- and lipopolysaccharide-stimulated lymphocytes compared with PBS or monotherapy treatments. Further western blotting analysis suggested that RES-lips may enhance the resistance of RCC to sorafenib by inhibiting PI3K-AKT-mTOR and VHL-HIF signaling pathways, ultimately augmenting the tumor growth inhibition effect of the combination therapy. RES-lips may improve the sorafenib resistance in RCC, and the underlying mechanism may be related to the regulation of PI3K-AKT-mTOR and VHL-HIF signaling pathways.

1. Introduction

As one of the top ten malignant tumors worldwide, RCC is a malignant tumor arising from the urothelium of renal parenchyma. Statistical data reveals a gradual increase in RCC incidence, with approximately 290,000 new cases diagnosed annually. Moreover, RCC accounts for about 2 % of global tumor mortality. Currently, the primary treatment approach for RCC is radical surgery. However, for patients who have developed distant metastasis, or when the tumor is too large and the local anatomy of the tumor growth site is complex, RCC exhibits resistance to radiotherapy and chemotherapy. In such cases, clinical practice primarily relies on targeted drugs as a supplementary treatment. Commonly used targeted drugs for RCC treatment in clinical settings include sorafenib, Sunitinib, and others.

* Corresponding authors at: Cancer Center, Department of Ultrasound Medicine, Zhejiang Provincial People's Hospital, Affiliated People's Hospital, Hangzhou Medical College, 158 Shangtang Road, Gongshu District, Hangzhou, Zhejiang, China.

E-mail addresses: 1320834133@qq.com (W. Chen), Ljc9702117@hotmail.com (J. Li), LTS201866@163.com (L. Sun).

[1] These authors contributed equally.

https://doi.org/10.1016/j.ijpx.2024.100280
Received 3 July 2024; Received in revised form 19 August 2024; Accepted 24 August 2024
Available online 26 August 2024

Sorafenib is a multi-tyrosine kinase inhibitor (TKI)that exerts its antitumor effects through dual mechanisms. It not only directly inhibits tumor cell proliferation by blocking the RAF/MEK/ERK-mediated cell signaling pathway but also suppresses tumor neovascularization by inhibiting VEGFR and platelet-derived growth factor (PDGF) receptors, and indirectly inhibiting tumor cell growth (Escudier et al., 2019; Shi et al., 2011; Sun et al., 2022). TARGET is a Phase 3 trial of patients with advanced RCC, and the results showed that the median PFS was 5.5 months *vs.* 2.8 months in both groups of patients (sorafenib *vs.* placebo) and 26.3 weeks *vs.* 13.9 weeks in both groups of patients ≥70 years of age (sorafenib *vs.* placebo) (He et al., 2021). In December 2005, the US FDA approved sorafenib for the treatment of patients with unresectable renal cancer (Kane et al., 2006). In 2006, sorafenib opened the door to targeted therapy for advanced renal cancer as the first molecularly targeted drug for renal cancer to enter the Chinese market (Yang et al., 2012). However, while sorafenib initially induces tumor regression, acquired resistance gradually develops, leading to ineffective treatment in some patients (Oya et al., 2022). There are many studies on sorafenib resistance-related signaling pathways (Li et al., 2023). It has been found that RCC cells can induce the development of primary resistance to sorafenib by upregulation of EGFR and its ligands leading to sustained activation of the downstream pathway Ras/Raf/MEK/ERK (Cui et al., 2016). Therefore, exploring novel therapeutic targets or combination strategies to prevent tumor progression and sorafenib resistance is a pressing concern in the treatment of RCC.

The combination of chemical drugs with traditional Chinese medicine (TCM) presents a promising approach to enhance antitumor activity, manage adverse reactions, and prevent the emergence of drug resistance by acting on multiple pathways simultaneously (Jiashuo et al., 2022). Therefore, the combination of TCM and sorafenib to improve the overall efficacy of RCC by improving its drug resistance is a very promising research direction (Lee et al., 2022). Resveratrol (RES), a naturally occurring polyphenol and phytotoxin, is widely distributed in grapes, berries, peanuts and other plants, and has anti-inflammatory, anti-oxidant, anti-cancer and neuroprotective effects (Zhu et al., 2022). Recent reports revealed that RES holds promising antitumor activity and is safe to normal cells (Tian et al., 2020; Zhu et al., 2022).

However, as a drug molecule, RES's monomeric form suffers from poor *in vivo* stability due to its small molecular weight, which can hinder its antitumor potential (Zhu et al., 2022). In recent years, as a new drug carrier, liposomes are mainly composed of phospholipid bilayer membranes, with cell-like bilayer structure, hydrophilic and lipophilic molecules (Guimarães et al., 2021). Many studies have found that liposome encapsulation can improve the physicochemical properties, stability and bioavailability of the drug (Akkewar et al., 2023). Kristl et al. found that RES liposomes could delay drug release, enhance cell absorption and effectively avoid free radical damage (Zupančič et al., 2015). Similarly, Ethemoglu et al. found that liposome encapsulation improved the stability of free RES in epileptic rats, enhancing its therapeutic effect and antioxidant and antiepileptic properties(Ethemoglu et al., 2017).

Consequently, the antitumor potential of RES in malignant tumors has garnered increasing attention. Our previously published study have also shown that RES achieves synergistic antitumor activity in synergy with sorafenib (Wang et al., 2023). However, the role and mechanism of RES in improving resistance to sorafenib in the treatment of RCC are unknown. The primary objective of this study was to investigate the antitumor activity of RES and elucidate the potential mechanism underlying its ability to improve sorafenib resistance in RCC.

2. Material and methods

2.1. Materials

Resveratrol with a purity greater than 98 % was brought from Shanghai Source Biotechnology Co., Ltd., and sorafenib was purchased from Beijing Solarbo Biotechnology Co., Ltd. (purity: 99 %). mTOR pathway activator MHY1485 and dimethyloxy glycine (DMOG) were purchased from Wuhan Purity Biotechnology Co., LTD. RE-2000 rotary evaporator was introduced by Shanghai Yarong Biochemical Instrument Factory. Micropipettes (Eppendorf, Germany); CPS2 ultrasonic pulverizer (Ningbo Xinzhi Ultrasonic Co., Ltd.); 85–2 Thermostatic magnetic stirrer (Changzhou Ouhua Instrument Co., Ltd.); TGL-18-B High Speed Centrifuge (Hunan Xingke Instrument Co., Ltd.); U-3010 Ultraviolet-Visible Spectrophotometer and JEM100SX Transmission Electron Microscopy (TEM) (Hitachi, Japan). CCK-8 kit, RPMI-1640 medium and FBS, trypsin and DMEM medium were obtained from Thermal Fisher Scientific. RIPA lysate was purchased from Beijing Solarbo Technology Co. , Ltd. Other conventional reagents, such as Tween-20, BSA, PMSF and glycine, were purchased from Sigma-Aldrich. All renal cancer cells, including sorafenib-resistant cells, were purchased from Beijing Jinye Biotechnology Co., Ltd. Primary antibodies were purchased from Abcam Technology, including targeting PI3K/AKT/TOR signaling pathway panel (ab283852) , HIF-1 alpha (ab279654) , Bcl-2(ab182858), BAX (ab32503) ; VEGF (ab150375) , PDGF(ab178409) , EGF(ab184265).

2.2. Preparation and quality detection of RES-lips

RES-lips suspensions were prepared using the rotary thin-film evaporation-sonication method. Accurately weigh the lecithin to cholesterol mass ratio (mPC: mChol = 5: 1, 8: 1, 10: 1, 12: 1), drug-to-lipid ratio (mass ratio of RES to lecithin: mRES: mPC = 1: 25, 1: 40, 1: 50, 1: 60), add an appropriate amount of absolute ethanol to dissolve, transfer it to a round-bottom flask, and rotate on a rotary evaporator at 45 °C until ethanol is completely evaporated completely and a uniform and transparent film is formed. The RES-lips suspension was obtained by pouring 10 mL of phosphate buffer solution (PBS, pH = 7.4) into the above round bottom flask for hydration and membrane washing. After sonication on a water bath, the suspension was placed in a dialysis bag, protected from light, and the unencapsulated RES was removed.The resulting product, RES-lips, was sealed and stored in a refrigerator at 4 °C for further use.

The morphology and particle size distribution of RES-lips were determined using transmission electron microscopy and laser particle size analyzer, respectively. A drop of freshly prepared RES-lips suspension was pipetted onto the surface of the coated copper mesh, dried naturally, and then the liposomes were negatively stained with 4 % phosphotungstic acid solution for 30 s. Finally, the air-dried copper mesh was placed on the transmission electron microscope to observe the microscopic morphology of RES-lips. For particle size measurement, the RES-lips suspension was diluted 10-fold with secondary water, sonicated, and the particle size was measured using a laser particle size analyzer.

The entrapment efficiency of RES-lips was determined as follows: A series of concentration gradient RES standard solutions were prepared, and the absorbance at the maximum absorption wavelength of 306 nm was measured using an ultraviolet spectrophotometer. A standard curve of absorbance *versus* concentration was then plotted. The absorbance value of the dialysate of RES-lips (mPC: mChol = 10:1, mRES: mPC = 1:40) at 306 nm was measured using an ultraviolet spectrophotometer, and calculate the corresponding RES content by substituting the calibration curve equation. The formula for calculating the entrapment efficiency (% EE) of RES-lips is as follows: % EE = (1 − content of free RES in dialysate/total amount of initially added RES) × 100 %.

2.3. Experimental cell culture and animal husbandry

Human RCC cell lines were used *in vitro* using DMEM medium and McCoy's 5 A medium, respectively. Both media were supplemented with 10 % fetal bovine serum (FBS), 100 U/mL penicillin, 0.1 mg/mL streptomycin. Cells were cultured in a humidified cell incubator at 37 °C, 5 % CO_2. When the cells reached more than 80 % confluence in the microscopic field of view the cells were passaged. The waste from the flask was

first discarded, rinsed twice with PBS, then 2–3 mL of trypsin was added, digested in a cell incubator for 1–2 min, then trypsin was neutralized with 10 % serum medium, and the cells were beaten with a dropper and placed in a 15 mL centrifuge tube. Place the centrifuge tube into a centrifuge and balance, rotate at 800 rpm and centrifuge for 5 min. Discard the waste after centrifugation for passage.

SPF grade, 4-week-old male M-NSG and WT mice were purchased from Shanghai Model Biology Center (China). Mice were housed in an SPF-grade environment and housed in light and dark for 12 h.All experiments were accredited by the Ethics Committee in accordance with care and use in facilities accredited by the International Association for Assessment and Accreditation of Laboratory Animals (AAALAC), standard food and water were provided.

2.4. Detect the proliferation-toxicity of RES-lips and sorafenib on RCC via CCK-8 assay

Cells in the logarithmic growth phase were seeded in 96-well plates at a density of 5E4/mL with 100 μL of medium per well. After the cells reached 80 % confluence, different concentrations of RES-lips (6.25, 12.5, 25, 50, 100, 200, 400, 800 mg/L) prepared in complete culture medium were added to the wells using the gradient dilution method. A blank control group (cells+culture medium, without RES-lips supplement) was set up in triplicate wells in each group. Set up another zero adjustment well (culture medium). The 96-well plate was placed in a cell incubator (37 °C, 5 % CO_2) for 48 h, and the liquid in each well was discarded, 100 μL of culture medium containing 10 % CCK-8 was added to each well, and incubated in the incubator for 4 h. The absorbance value (A) of each well at 450 nm was measured with a plate reader. The cell survival rate (%) = (mean A of test group-mean A of blank control)/(mean A of control group-mean A of blank control) × 100 % was used to calculate the effect of each group on the survival rate of both types of cells and the corresponding IC50 value. The proliferation-toxicity effect of sorafenib on cells was determined using the same steps with the action concentrations of 3, 6, 12, 24, 48, 96, 192 μmol/L and 15, 30, 60, 120, 240, 480, 960 μmol/L, respectively. The combined index (CI) was calculated with reference to previously published articles, and CI < 0.9 had a synergistic effect.

2.5. Plate clonogenic assay

Cells in the logarithmic growth phase were digested, resuspended, and counted. The cell suspension density to 1E4 cells/well, seed in a 6-well plate, and incubate in a humidified cell incubator at 37 °C and 5 % CO_2 for 24 h. Subsequently, different concentrations of drug were added to each well, and the culture was continued for 48 h, followed by fluid exchange and drug withdrawal. After 2 weeks of continuous culture, the culture medium in the wells was aspirated, fixed in 4 % paraformaldehyde for 2 h, and then stained with crystal violet solution for 12 h as directed. The crystal violet solution was removed, rinsed carefully twice with deionized water, and allowed to dry.

2.6. Migration test

Cells in the logarithmic growth phase were seeded in 6-well plates and placed in a humidified cell incubator at 37 °C and 5% CO_2. When the cells are almost full of the 6-well plate, a scratch was made from top to bottom using a 10 μl tip, keeping the tip vertical during the scratch. After scratching, the cells were washed twice with PBS. Subsequently, serum-free medium (control group) and serum-free medium combined with different drugs were used for culture. Photographs were taken 24 h later, and the width between cells was observed and measured by fluorescence inverted microscope. Cell migration distance = (0 h intercellular distance – 24 h migration distance)/2.

2.7. Invasion test

The Matrigel was thawed in a refrigerator at 4 °C overnight and diluted in pre-cooled medium according to the instructions. Subsequently, it was spread in a Transwell chamber, coagulated at room temperature, and 50 μL of the basement membrane hydrated with 10 g/L bovine serum albumin was added before the experiment, and then placed at 37 °C for 30 min. Cells were withdrawn from serum for 12 h, then digested and counted, resuspended in serum-free medium, and the concentration was adjusted to 1E5/ml. 200 μL of the cell suspension was added to each chamber and 10 % serum medium was added to the lower chamber. Cells were cultured at 37 °C and 5 % CO_2 for 24 h. The chambers were removed, washed twice with PBS, fixed in 4 % paraformaldehyde for 2 h, and stained with 4 g/L crystal violet solution for 2 h. Photographs were taken, and cells were counted under a microscope.

2.8. Tumor model establishment and experiment

The mouse RCC tumor model was established using 786-O/S cells. Cryopreserved 786-O/Scells were first taken and incubated in 1640 medium in a 37 °C, 5 % CO_2 incubator for 48 h. Cells in the logarithmic phase of growth were taken, washed after harvest, then PBS was added to a concentration of 5E6 cells/mL. Mice were incubated adaptively in the SPF animal room for 1 week prior to enrollment and 0.2 mL of 786-O/Scells were injected into the axilla of each mouse. After the tumor grew to 60–80 mm^3, mice were divided into 4 groups, receving the treatment of PBS (Model control group), RES-lips (RES-lips group) and Sorafenib alone (Sorafenib group) or combination (Combination group), respectively, according to the mean tumor size and body weight. Tumor-bearing mice in the model control group were given 500 μL of PBS daily by gavage; Those mice received the treatment of two monotherapy were given 20 mg/kg and 200 μmol/kg Sorafenib and RES-lips once daily by gavage, respectively; Sorafenib (20 mg/kg) and RES-lips (200 μmol/kg) were administered daily by gavage to tumor-bearing mice. All tumor-bearing mice were treated for 14 consecutive days.

The length (L) and width (W) were measured using a conventional caliper in mice, and the tumor volume was calculated as $V = 0.52 \times L \times W^2$ in cubic millimeters. Tumor growth inhibition rate (TGI) was calculated as: TGI = (1-tumor volume in the treatment group/tumor volume in the control group) *100 %.

At the end of the experiment, the spleens of tumor-bearing mice in each group were sacrificed and separated into RPMI-1640 medium after grinding. After adjusting the cell concentration to 1E7, the spleen was adjusted to a 96-well cell culture plate, 100 μL per well, and the final concentration of ConA was 2.5 μg/mL, and then incubated in 37 °C and 5 % carbon dioxide incubators for 2 days.3.5 h before the end of the culture, detection agents diluent at a final concentration of 1 mg/mL was added to continue the incubation for 2 days, then lymphocytes were centrifuged, resuspended in 100 μL DMSO, and the OD values at 570 nm were measured after sufficient shaking.

2.9. Ex-vivo lymphocyte proliferation test

After cervical dislocation of mice in each drug-treated group was sacrificed, the spleen was aseptically removed, the spleen was ground in a mortar, and the cell suspension was transferred into a plastic centrifuge tube; centrifuge at 2000 r/min for 5 min, mix well with 1 mL RPMI-1640 medium and count;Adjust the cell concentration to 107 cells per mL, and add 100 μL per well to A 96-well cell culture plate [containing 3.0 μg/mL of ConA or 5.0 μg/mL of lipopolysaccharide (LPS). Place the 96-well cell culture plate into A cell incubator at 37 °C.Incubation was continued with 5 % CO_2 for 2 days. At 4 h before the end of culture, 50 μL of MTT diluent (2.0 mg/mL) was added to each well, the culture was continued until 48 h, 3000 r/min, centrifuged for 10 min to precipitate lymphocytes, and the cell culture medium was gently decanted.The optical density values (OD) were determined at a detection wavelength

of 570 nm after addition of DMSO and well were shaken thoroughly.

2.10. Western blotting assay

Tissues from tumor bearing mice were collected from each group of tumor-bearing mice ($n = 3$). This tissues were further weighed, and the tissue lysate was added in a ratio of 1: 10. After homogenization for 1 h on ice, the samples were centrifuged at 12000 *g*, 10 min at low temperature to obtain supernatant.The protein concentration in the supernatant was subsequently quantified by BCA method. Based on the BCA quantification results, 25 μg of the corresponding total protein was subjected to SDS-PAGE electrophoresis based on the quantitative results of BCA, followed by gel transfer onto PVDF membranes. Block with skim milk for 1 h, then add primary antibodies against different targets (antibody dilutions ranging from 1: 5000 to 1: 10,000) and incubate in a refrigerator at 4 °C overnight.After the pvdf membrane was washed the next day, substrate was added and detected and photographed using a bioimaging system. The analysis software of the system was used to analyze the gray value.

2.11. Statistical analysis

Data analysis was performed using SPSS software (Version No. 22.0). All data are presented as mean ± standard deviation (SD). The effects of RES-lips, sorafenib at different concentrations and different concentrations of RES-lips in combination with sorafenib on the proliferation of cancer cells were analyzed by ANOVA one-way analysis of variance and Dunnett's *post hoc* test. The *t*-test was used to compare the effects of RES-lips on the expression of signal pathway-related proteins or mRNA. A *P*-value <0.05 was considered statistically significant.

3. Results

3.1. Preparation of RES-lips and determination of quality parameters

RES-lips were observed macroscopically as a homogeneous milky-white suspension. Cryoelectron microscopy revealed a homogeneous distribution of RES-lips with a roughly spherical shape. The mean particle size of RES-lips as detected by a nano-laser particle size analyzer was 102.1 ± 10.5 nm, PDI was 0.244, and Zeta was −12.82 mV, respectively. The encapsulation efficiency (EE) of RES-lips was determined to be 91.2 ± 5.1 %, indicating effective encapsulation of RES.

3.2. Inhibitory effects of RES-lips and sorafenib on proliferation of different RCCs

The cytotoxicity of RES-lips and sorafenib, alone or in combination, on 786-O/S and 786-O cells (sorafenib-resistant and normal renal cell lines, respectively) was tested by CCK-8 assay, with HEK293T cells used as a control. As the results showed in Figs. 3A-B, sustained increases in RES-lips or sorafenib concentrations in the range of 5–320 mmol/L and 4–128 μmol/L, respectively, exhibited no significant effect on the cell viability of HEK293T cells compared to control. Moreover, CCK-8 assay also demonstrated that different concentrations of RES-lips or sorafenib inhibited the proliferation of 786-O/S and 786-O cells in a dose-dependent manner. The IC_{50} of sorafenib to 786-O and 786-O/S was 1.6 ± 0.2 μmol/L and 23.1 ± 5.2 μmol/L, respectively. The IC_{50} of sorafenib-resistant strains was significantly higher. The RI of 786-O/S cells to sorafenib was calculated to be 14.4 based on the resistance index (RI) = IC_{50} (resistant cells)/IC_{50} (parental cells). (See Figs. 1 and 2.)

3.3. RES-lips reversed the resistance of 786-O/S cells to sorafenib

We further treated 786-O/S cells with different concentrations of RES-lips in combination with 23.1 ± 5.2 μmol/L sorafenib. As shown in

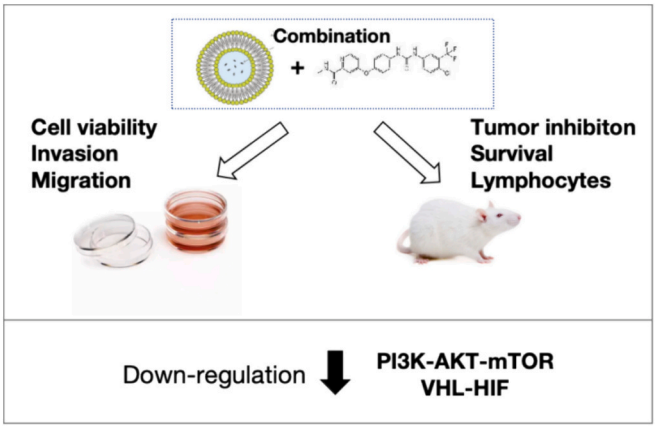

Fig. 1. Schematic of the efficacy and mechnism of RES-lips combined with sorafenib for anti-RCC therapy.

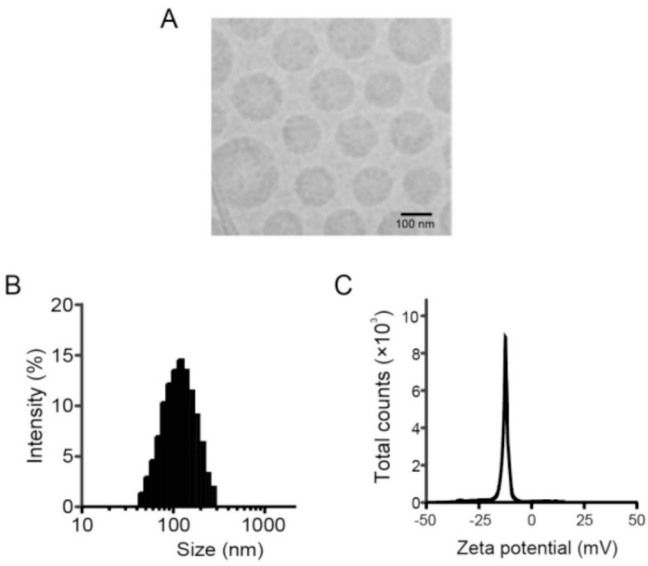

Fig. 2. Characterization of Sem-PEG-lips. (A) scanning electron microscopy; (B) particle size distribution and (C) zeta potential of Sem-PEG-lips.

Fig. 4A, no significant difference in the cell viability between the addition of 1, 2, 4, and 8 mmol/L RES-lips in combination with sorafenib and 786-O/S with sorafenib alone. Renal carcinoma cell viability was shown to be more significantly reduced at 16 and 32 mmol/L (both $P < 0.001$). When the concentration of RES-lips was increased to 16 mmol/L, the sensitivity of 786-O/S cells to sorafenib was significantly enhanced, and the inhibition of sorafenib on the viability of 786-O/S cells was enhanced. According to the relative reverse rate (RRR) = [IC_{50} (chemotherapeutic agent of resistant strain alone)-IC_{50} (chemotherapeutic agent of resistant strain + reversal agent)]/[IC_{50} (chemotherapeutic agent of resistant strain alone) -IC_{50} (parental strain alone)], RRR ≥ 1 represents complete reversal, RRR < 1 represents partial reversal, and RRR of RES-lips is 0.58.

The CI values for each concentration of the drug when coadministered were further calculated and the results are shown in Fig. 4B. The results of RES-lips at 4–32 mmol/L and sorafenib at 23.1 mmol/L were 1.38, 0.77, 0.41 and 0.32, respectively, which were all less than 1, suggesting a synergistic inhibitory effect on the proliferation of the sorafenib-resistant renal cancer cell line.

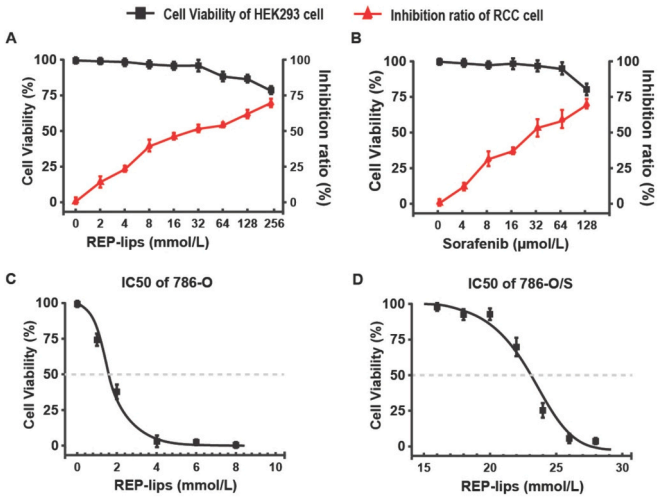

Fig. 3. Evaluation of the inhibitory effects of RES-lips and sorafenib on the proliferation of different RCCs. Effects of (A) sorafenib and (B) RES-lips alone on the activity of HEK293T and renal cell; Effect of Sorafenib on the viability of (C) sensitive strain 786-O and (D) resistant strain 786-O/S renal carcinoma cells. All data are expressed as mean ± SD ($n = 6$).

3.4. RES-lips in combination with sorafenib significantly suppress the invasion and migration of RCC cells

As shown in Fig. 5, the invasion and migration of sorafenib-resistant RCC cells, 786-O/S cells, were investigated after one day of treatment of sorafenib and RES-lips alone or combination. The 786-O/S cells incubated with sorafenib combined RES-lips exhibited the shortest 24 h-migration distance than other treatment groups, and the healing area was significantly lower than controls and both monotherapy groups. Moreover, the effect of sorafenib and RES-lips on the invasive capacity of 786-O/S cells are evaluted and results were showed in Fig. 5B. The number of perforated cells in the individual field of the combination therapy group was significantly lower than that in the control and both two monotherapy incubation groups. These results collectively suggested that sorafenib and RES-lips can effectively suppress the invasion and migration of sorafenib-resistant RCC cells.

3.5. RES-lips combined with sorafenib significantly enhanced G1/S arrest in RCC cells

We further investigated whether RES-lips in combination with

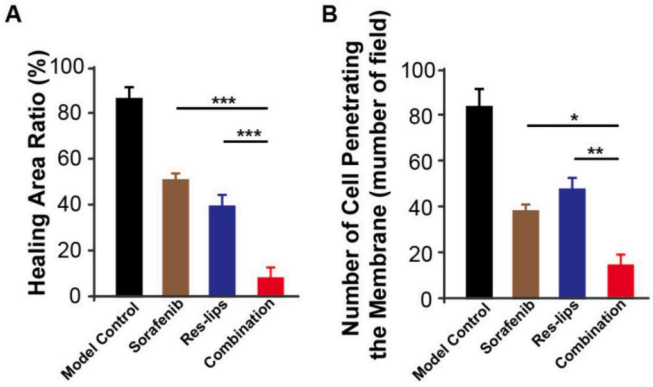

Fig. 5. Effects of sorafenib and RES-lips alone or in combination on (A) migration and (B) invasion of RCC cells. (*, **, ***) $P < 0.05$, 0.01, 0.001 compared with the negative control group.

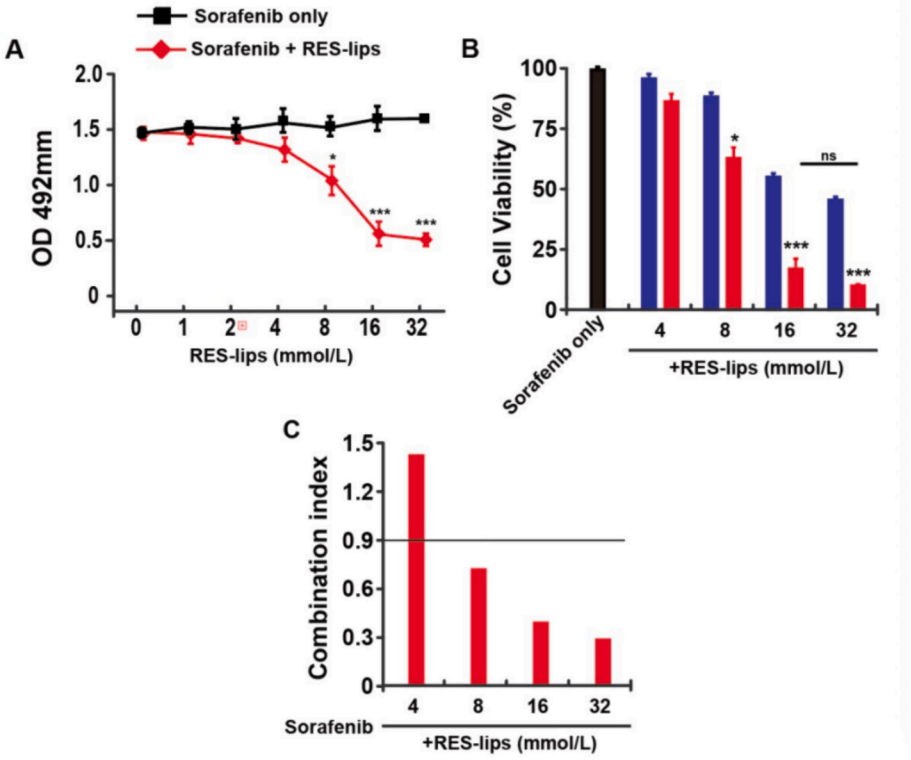

Fig. 4. Inhibition of RES-lips combined with sorafenib on the viability of drug-resistant cells in renal carcinoma. (A)-(B) The effect of sorafenib combined with RES-lips on the viability of 786-O/S renal carcinoma cells and (C) The CI value of sorafenib combined with RES-lips on the proliferation of renal carcinoma cells was analyzed by CompuSyn software. Using one-way analysis of variance (*, ***) $P < 0.05$, 0.001 *vs.* Sarafenib only. All data are expressed as mean ± SD ($n = 6$).

sorafenib can promote cell cycle arrest in RCC cells. As shown in Fig. 6, compared with the sorafenib monotherapy group, after administration of RES-lips in combination with sorafenib, 786-O/S was significantly arrested in G1 phase, the proportion of cells in G1 phase was significantly increased (79.39 % *vs.* 43.86 %, $P < 0.01$), and the proportion of cells in S phase was significantly decreased (11.25 % *vs.* 38.36 %, $P < 0.01$). It was suggested that RES-lips combined with sorafenib resulted in 786-O/S cell arrest in G1/S phase. In addition, compared with the high-dose sorafenib monotherapy group, the G1/S phase block effect in the combination group was significantly greater.

To better understand the mechanism by which this combination inhibits the G1/S transition, we examined the expression of several key regulatory factors involved in this process, including CDK4, CDK6, Cyclin D, CDK2, Cyclin E, and p-Rb. As shown in Fig. 7, among all these protein markers, the expression levels of CDK6, CDK2, pRb were lower and the expression levels of Cyclin E and Cyclin D were higher in the combination group, partially suggesting G1/S phase arrest. Taken together, our results clearly demonstrated that RES-lips in combination with sorafenib can significantly enhance G1/S arrest in sorafenib-resistant RCC cells.

3.6. *RES-lips reverses sorafenib resistance in a sorafenib-insensitive RCC xenograft model*

The mouse xenograft model using screened 786-O/S cells resistant to sorafenib were successfully established, and the dosing design of sorafenib and RES-lips in animal experiments was shown in Fig. 8A. Once the tumor size of mice reached 80–100 mm^3, the mouse renal carcinoma model was deemed successful and initiated treatment. The tumor growth of mice in each treatment group was shown in Fig. 8B. Although the tumor size of mice in the sorafenib monotherapy group was significantly decreased compared to the model control group, there was no statistically significant difference ($P < 0.05$), with TGI of only 29.2 %, and no animal achieved CR. Notably, the combination of RES-lips with sorafenib significantly inhibited the growth of mouse renal tumors relative to the model control group ($P < 0.001$), achieving a TGI of 90.1 % on Day 35, of with three mice achieving complete tumor response. Furthermore, TGI was also significantly higher in mice treated with the combination than in the RES-lips (53.6 %) and sorafenib (29.2 %) monotherapy groups (both $P < 0.01$). In terms of tumor-bearing mouse survival, the survival rate was 100 % in the combination of sorafenib and RES-lips compared with 16.6 %, 33.3 %, or 66.7 % in the negative control, sorafenib, or RES-lips monotherapy groups, respectively. These results collectively suggested that combination therapy achieves significantly better antitumor effects in a sorafenib-sensitive RCC xenograft model.

3.7. *Effect of RES-lips combined with sorafenib on lymphocyte proliferation in sorafenib-insensitive RCC model mice*

We further used lymphocyte proliferation assay to observe the effect of RES-lips combined with sorafenib on lymphocyte proliferation in RCC. At the end of the *in vivo* efficacy study, spleens from mice treated with RES-lips and sorafenib alone or in combination were removed under aseptic conditions for use in an *in vivo* lymphocyte proliferation assay. As shown in Fig. 9, compared with the vehicle control group, splenocyte proliferation was increased in the RES-lips group ($P < 0.05$), while the sorafenib group showed some inhibitory effect on lymphocyte proliferation after both unstimulation and Con A stimulation ($P < 0.05$). The combined treatment with RES-lips and sorafenib alleviated the inhibitory effect of sorafenib on lymphocyte proliferation, which was significantly superior to the sorafenib alone group ($P < 0.05$). For LPS-stimulated splenic lymphocytes, the combination slowed the inhibitory effect on LPS-stimulated splenic lymphocytes ($P < 0.05$ *vs.* vehicle control). The results showed that the combination of RES-lips and sorafenib could promote the proliferation of splenic lymphocytes and enhance the inhibitory effect of sorafenib on the proliferation of splenic lymphocytes.

3.8. *RES-lips improved the resistance of sorafenib in RCC models by regulating PI3K-AKT-mTOR and VHL-HIF signaling pathways*

To investigate the mechanism of RES-lips combined with sorafenib on RCC, Western blot was used to detect the changes of protein levels in tumor samples of each group. The results showed that RES-lips enhanced the inhibitory effect of sorafenib on the expression of PI3K-AKT-mTOR signaling pathway-related proteins, and the expression level of related proteins was significantly lower than that of sorafenib alone (Fig. 10). Moreover, RES-lips significantly regulated the expression of VHL-HIF axis-related proteins, *i.e.* up-regulated the expression of VHL protein, and then inhibited the up-regulation of HIF-a, VEGF, PDGF, EGF and other growth factors. Considering that PI3K-AKT-mTOR and VHL-HIF signaling pathways affect tumor cell survival, growth, metabolism, as well as tumorigenesis and metastasis, they play a key role in the resistance process of renal tumors to sorafenib, RES-lips can achieve reversal of sorafenib resistance. Moreover, RES-lips reversed the decreased Bcl-2 levels and upregulated BAX levels with sorafenib, whereas the trend of protein expression after RES-lips combined with sorafenib was similar to that of sorafenib, *i.e.*, decreased Bcl-2 expression and increased BAX expression (Fig. 11).

In the rescue experiment, we observed that the introduction of mTOR pathway activator (MHY1485) or HIF agonist dimethyloxy glycine (DMOG) could significantly reduce the survival rate of tumor-bearing

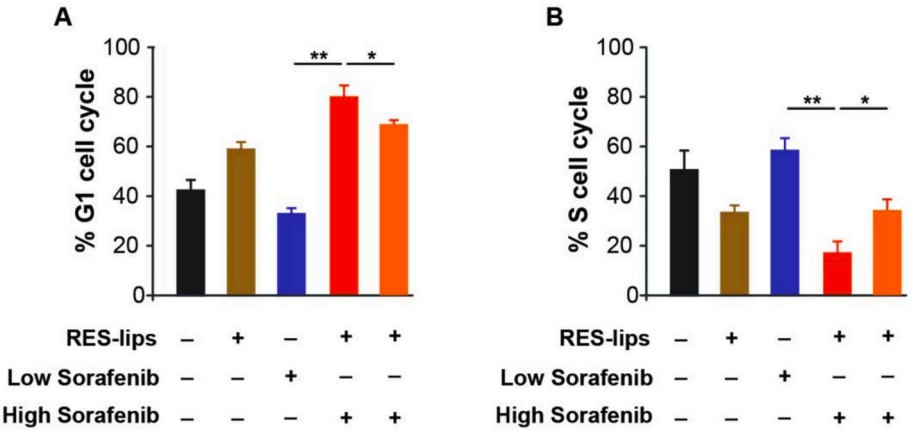

Fig. 6. Effect of different drug treatments on cell cycle arrest of RCC. (A) Proportion of cells in G1 phase and (B) proportion of cells in S phase. (*) and (**) *vs.* $p < 0.05$ and 0.01 were used. Control group or sorafenib combined with RES-lips group.All data are presented as mean ± SD ($n = 6$).

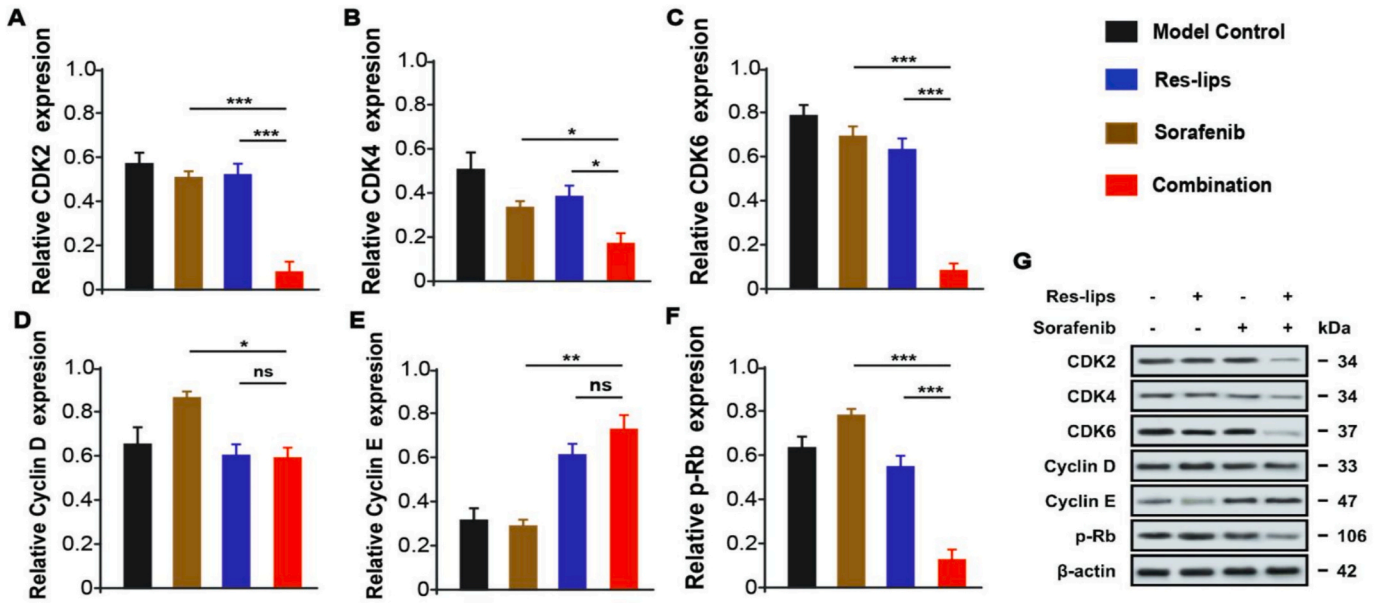

Fig. 7. Effects of different drug treatments on the expression of cell cycle-related proteins in RCC. (A) CDK-2; (B) CDK-4; (C) CDK-6; (D) Cyclin D; (E) Cyclin E, (F) p-Rb expression levels and (G) representative WB gel images. (*,**,***) *vs.* $p < 0.05$, 0.01, 0.001. All data are presented as mean ± SD (n = 6).

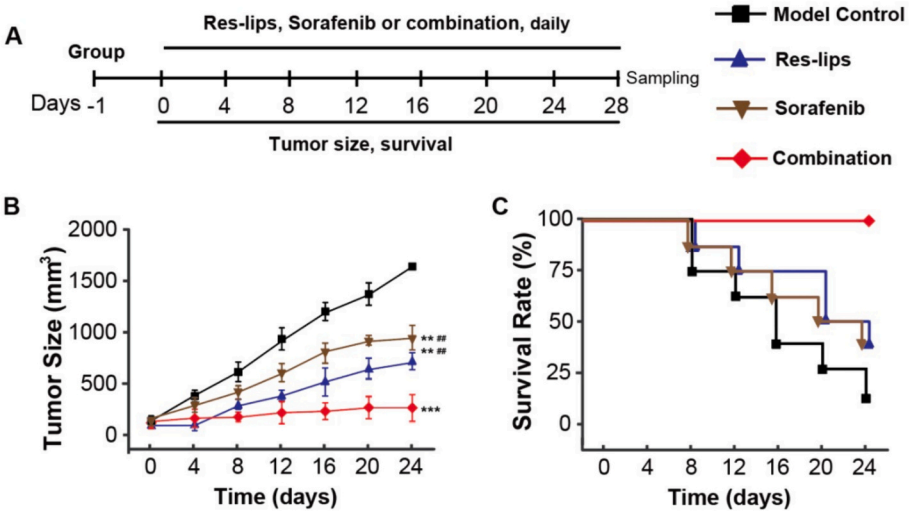

Fig. 8. Therapeutic effects of different drug treatments on sorafenib-resistant RCC model mice. (A) animal dosing flow charts, (B) tumor size, and (C) survival rate of tumor-bearing mice. (**) and ($^{\#\#}$) $p < 0.01$ *vs.* control group or sorafenib combined with RES-lips group. All results are presented as mean ± SD ($n = 8$).

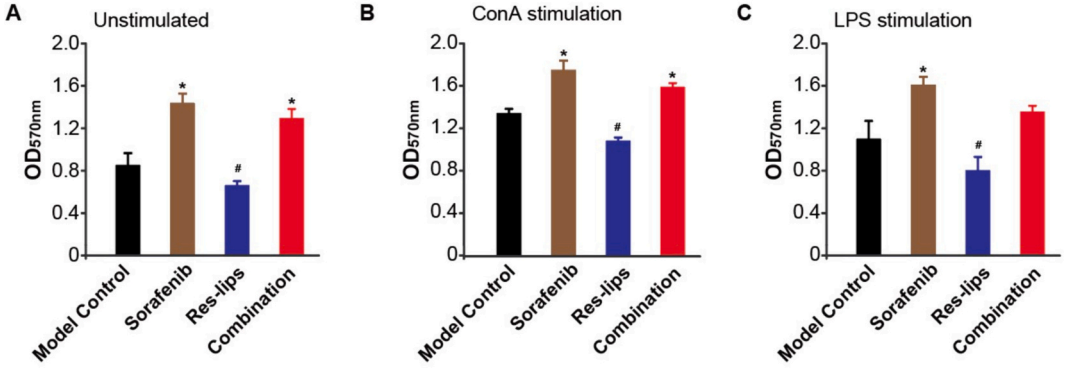

Fig. 9. Effect of RES-lips combined with sorafenib on lymphocyte proliferation. (*) and ($^{\#}$) $P < 0.05$ *vs.* control group or sorafenib combined with RES-lips group.

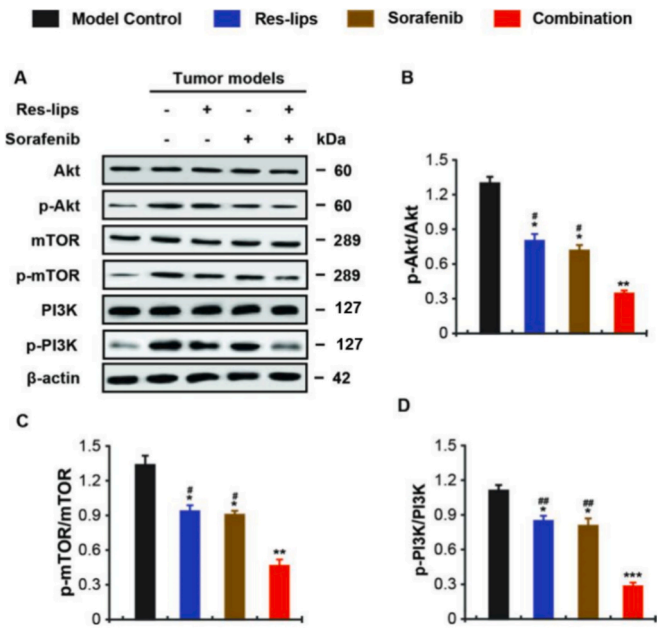

Fig. 10. Effect of combination therapy on protein expression of sorafenib resistance-related signaling pathways in RCC xenografts. (A) Western blot gel imaging and (B)-(D) quantitative analysis. All data are presented as Mean ± SD ($n = 3$). Using (*, **) and ($^{\#}$, $^{\#\#\#}$) $P < 0.05$, 0.01 *vs.* control group or sorafenib combined with RES-lips group.

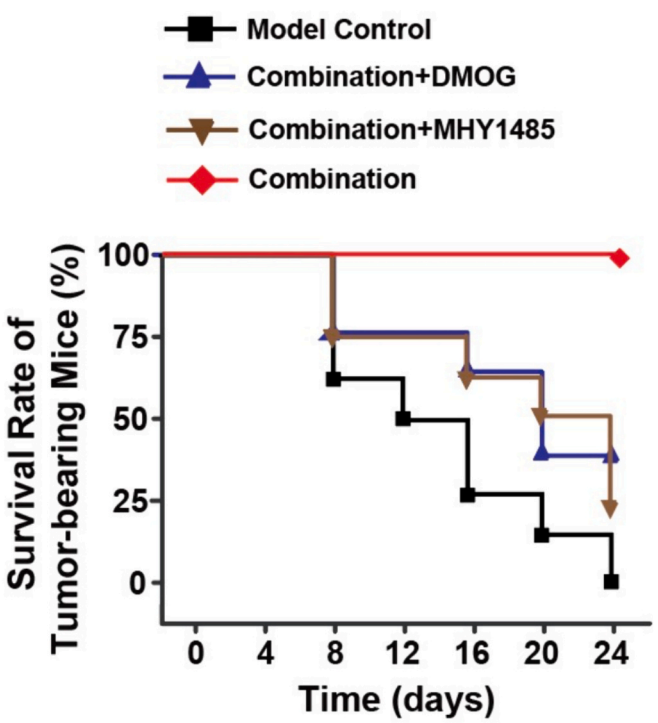

Fig. 12. Figure. Survival rate of sorafenib-resistant RCC model mice in rescue experiment. All results are presented as mean ± SD ($n = 8$).

mice in the combination therapy group (Fig. 12). These results collectively demonstrated that the RES-lips may improve the resistance of sorafenib to RCC cells by inhibiting PI3K-AKT-mTOR and VHL-HIF signaling pathways, inhibiting tumor angiogenesis and affecting the expression of apoptotic proteins, thereby enhancing the growth inhibitory effect of the overall combination therapy.

4. Discussion

Renal cell carcinoma (RCC), one of the top ten malignant tumors worldwide, is characterized by high morbidity and mortality, with China having the second highest incidence of urological neoplasms. RCC is often insidious at onset, and 30 % of patients have metastasized at diagnosis (Bahadoram et al., 2022; Msaouel et al., 2023). At present, the main treatment of RCC is surgery, adjuvant with conventional radiotherapy and chemotherapy, but for patients with advanced RCC who have distant metastasis have little effect (Bahadoram et al., 2022). Treatment is clinically supplemented with targeted agents, such as sorafenib, which is an oral small molecule multikinase inhibitor that

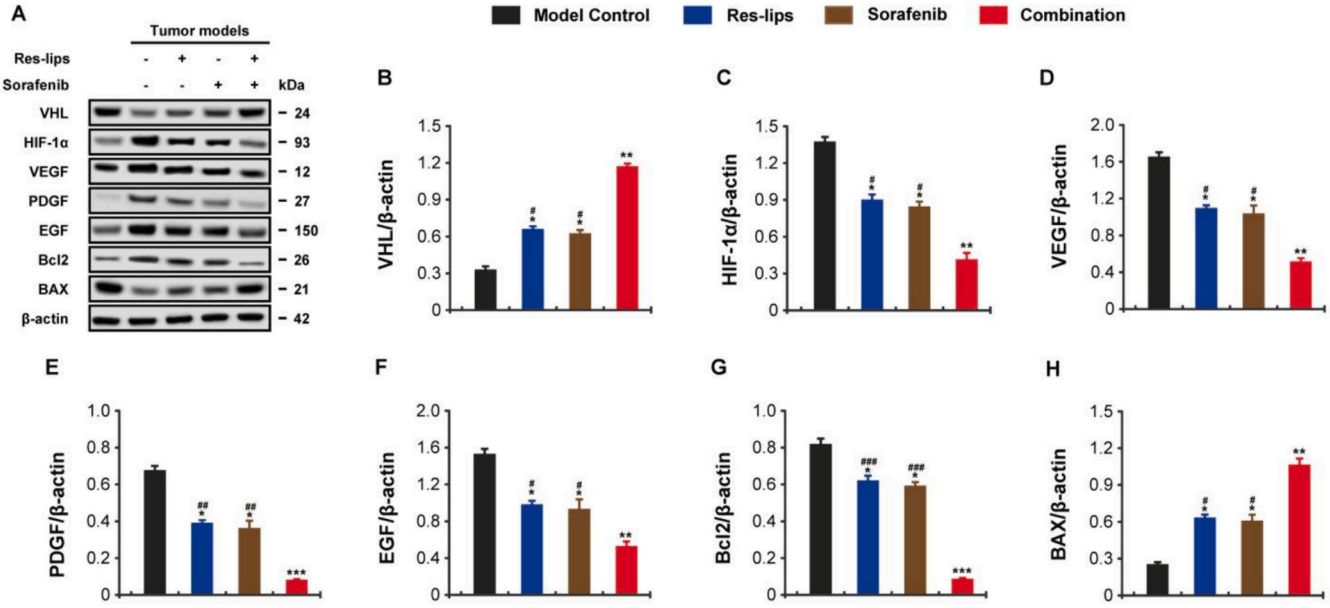

Fig. 11. Effect of combination therapy on VHL-HIF axis-related proteins and apoptosis-related proteins in renal carcinoma cell xenografts. (A) Western blot gel imaging and (B)-(D) quantitative analysis. All data are presented as Mean ± SD (n = 3). (*, **, ***) and ($^{\#}$, $^{\#\#}$, $^{\#\#\#}$) $P < 0.05$, 0.01, 0.001 *vs.* control group or sorafenib combined with RES-lips group.

inhibits tumor cell proliferation and growth by inhibiting the activities of c-RAF and b-RAF kinases and blocking RAF/MEK/ERK phosphorylation (Mei et al., 2014). Sorafenib can also block tumor neovascularization by inhibiting vascular endothelial growth factor receptor (VEGFR) and platelet-derived growth factor receptor (PDGFR) in endothelial and pericytes (Adnane et al., 2006). The introduction of targeted drugs has resulted in a significant survival benefit and a significant reduction in mortality in patients with RCC (Braun et al., 2021). However, 10 % to 20 % of RCC patients are innate resistant to sorafenib, and the remaining patients tend to develop resistance after 6 to 15 months of treatment, making sorafenib ineffective in prolonging their survival. (Chang et al., 2023). Therefore, exploring the biological mechanism of drug resistance to tumor-targeted drugs and enhancing the sensitivity of targeted drugs to patients has become a critical challenge for researchers.

Resveratrol, a natural monomer compound extracted from the roots of Veratrum trifolium, has shown anti-inflammatory, antioxidant, anti-tumor, metabolic regulation, and immunological activities. Modern pharmacological studies have found that resveratrol has anti-inflammatory, antioxidant, anti-tumor, metabolic regulation and immunological activities (Ren et al., 2021; Tian and Liu, 2020). Resveratrol can inhibit many kinds of tumor cells such as colon cancer, pancreatic cancer, ovarian cancer and breast cancer (Ren et al., 2021). Moreover, Resveratrol can exert anti-tumor activity by inhibiting tumor cell proliferation, inducing tumor cell apoptosis, inhibiting tumor cell invasion and metastasis, regulating immune function and directly acting on related targets (Chen and Musa, 2021). In addition, Resveratrol can also reduce the drug resistance of tumor cells to chemotherapeutic drugs and reverse multidrug resistance through ATP-binding cassette transmembrane transporter family, signal transduction pathway, SIRTl and apoptosis (Choi et al., 2022). Therefore, Resveratrol may be a drug that enhances chemosensitivity in RCC. It is not known whether Resveratrol will be used in the treatment of RCC in the future to reverse the multidrug resistance and improve the therapeutic effect of RCC caused by long-term chemotherapy. Therefore, we look forward to investigating the effects and potential mechanisms of their combination therapy in this study.

First, the RES-lips were prepared utilizing the rotary thin film evaporation-ultrasonic method, and measured the quality control indexes of RES-lips by cryo-electron microscopy and nano-laser particle size analyzer. The results obtained indicated that RES-lips exhibited uniform distribution, homogeneous size, and effective encapsulation of RES, rendering them suitable for further biological evaluations both *in vivo* and *in vitro*. Subsequently, we investigated the cytotoxicity of RES-lips and sorafenib alone or in combination on RCC cells, including both sorafenib-sensitive and -resistant cells, at the *in vitro* cellular level. RES-lips combined with sorafenib synergistically inhibited the proliferation of RCC cells, and the addition of RES-lips could reverse the resistance of 786-O/S cells to sorafenib. In clinical context, RCC represents most common renal tumor, and tumor metastasis is observed in approximately 15 % of patients (Huang and Becher, 2020). Renal cancer has the capacity to spread through blood vessels or lymphatics to distant organs, ultimately leading to death in a significant number of patients (Huang and Becher, 2020). Therefore, effective inhibition of metastasis and invasion in RCC is of paramount importance for controlling disease progression. In this study, RES-lips in combination with sorafenib significantly reduced the invasion and migration of 786-O/S cells. Drug treatment options for RCC include antiangiogenesis, immunotherapy, and mTOR pathway inhibition. Among them, mTOR is a highly conserved serine/threonine kinase from the PI3K-related kinase family and plays an important role in the regulation of cell growth, proliferation, and metabolism. Inhibition of mTOR results in a reduction in cell cycle progression, which in turn induces cell cycle arrest and apoptosis. For example, AZD8055, an experimental anticancer drug that also inhibits the activity of mTORC1/2, has been shown to achieve cell cycle arrest in RCC, effectively controlling the RCC. In this study, we also investigated the cell cycle arrest of RES-lips in combination with sorafenib in renal cancer cells. Current results suggested that RES-lips in combination with sorafenib result in 786-O/S cell arrest in the G1/S phase. Collectively, these findings demonstrate that RES-lips combined with sorafenib could effectively inhibit the activity of RCC cells and reverse sorafenib resistance, with a significantly better inhibitory effect compared to the two monotherapy groups.

Addition of RES-lips significantly enhanced the killing activity of sorafenib against RCC cells, particularly in sorafenib-resistant cell lines, within an *in vitro* model. To further evaluate the efficacy of this combination therapy, we employed a mouse xenograft model. Although the tumor size of mice in the sorafenib monotherapy group tended to decrease relative to the model control group, the TGI was less than 30 %, and no animals achieved complete remission. With the addition of RES-lips, the growth of renal tumors in the combination treatment group was significantly inhibited compared with the model control group (TGI: 90.1 %, $P < 0.001$), and 50 % (3/6) of the mice achieved complete tumor remission and the survival rate remained 100 %. In contrast, mice treated with either RES-lips or sorafenib monotherapy had significantly lower TGI or survival than the combination, suggesting a significantly superior antitumor effect of the combination therapy in a sorafenib-sensitive RCC xenograft model. However, the mechanisms underlying the RES-lips-mediated improvement of sorafenib resistance in RCC models require further elucidation.

The development or drug resistance of many cancers can be attributed to abnormalities in gene and protein levels (Makhov et al., 2018). Common mechanisms of resistance in RCC include gene mutations, signaling pathway abnormalities, cell cycle abnormalities, and disruption of cellular interaction environments (Jin et al., 2023). The VHL-HIF-hypoxia response gene pathway and PI3K/Akt/mTOR signal pathway, which plays a pivotal role in the regulation of cell cycle, are the main signaling pathways (Santoni et al., 2014). When PI3K/Akt/mTOR pathway is activated, cells will continue to proliferate and decrease apoptosis (Miricescu et al., 2021). Growth factors, cytokines and hormones, including VEGF, PDGF and EGF will activate PI3K, and then the activated PI3K phosphorylates phosphatidylinositol 4,5-bisphosphate, thereby transmitting the activated signal to downstream molecules (Massari et al., 2015). AKT is one of the main downstream targets and the activated AKT phosphorylates many substrates, thereby participating in the survival, growth, metabolism, tumorigenesis and metastasis of RCC cell (Miricescu et al., 2021). Abnormal activation of PI3K/Akt/mTOR pathway leads to the proliferation of cancer cells and the enlargement of lesions (Miricescu et al., 2021). Therefore, the abnormal activation of PI3K/Akt/mTOR pathway is closely related to the tumorigenesis and progression of RCC and resistance to sorafenib. Moreover, the stages of action of EGFR (HER1) and HER2 are both upstream of PI3K/Akt/mTOR pathway and affected by abnormal activation of signaling pathway (Miricescu et al., 2021). Thus, TKI inhibitors tend to lose therapeutic efficacy when patients develop aberrant activation of the PI3K/Akt/mTOR pathway. In this study, RES-lips significantly inhibited the upregulation of PI3K/Akt/mTOR signaling pathway-related proteins in RCC tissues, thereby mitigating the resistance of renal tumors to sorafenib.

Furthermore, research has demonstrated that the PI3K/Akt/mTOR signaling pathway can regulate the expression and translation of hypoxia-inducible factor-α (HIF-α), ultimately influencing TKI resistance (Badoiu et al., 2023). The HIF pathway is mainly related to VHL gene mutation, where the E3 ubiquitin ligase complex protein encoded by it targets HIF-α for degradation. This leads to continuous HIF activation, promoting angiogenesis, tumor cell growth, and transcription of downstream target genes (Zhang and Zhu, 2021). The corresponding platelet-derived growth factor (PDGF), vascular endothelial growth factor (VEGF) and epidermal growth factor (EGF) bind to the homologous tyrosine kinase receptor (RTK) on endothelial cells to promote tumor vascular growth (Zhang and Zhu, 2021). VHL gene deletion causes upregulation of HIF, which may in turn activate the mTOR

pathway after promoting the expression of a variety of growth factors including VEGF, PDGF, EGF, and subsequently activated mTORC1 and mTORC2 promote HIF expression, forming a positive feedback (Rasmussen and Rathmell, 2011). The expression of HIF-α was positively correlated with increased distant metastasis and decreased survival in different tumor types (Badoiu et al., 2023). In this study, RES-lips regulated the expression of VHL-HIF-signaling pathway-related proteins in RCC tissues, as evidenced by significantly reducing the accumulation of HIF-1α, thereby cooperating with the effects on PI3K/Akt/mTOR signaling pathway to achieve significantly enhanced antitumor activity and improved drug resistance, but further studies are needed to support this hypothesis. At the same time, the combination therapy also plays a common role in inhibiting tumor cell proliferation and tumor angiogenesis. Additionally, the combination therapy inhibited tumor cell proliferation and angiogenesis, promoted BAX expression, and reduced Bcl-2 levels, resulting in a more pronounced antitumor effect than RES-lips or sorafenib monotherapy.

Sorafenib resistance remains a significant challenge in advanced renal cancer treatment, necessitating the exploration of new multi-target and personalized therapies. Targeting PI3K/AKT/mTOR and VHL/HIF is not an effective long-term strategy against RCC. Because activation of PI3K/AKT/mTOR channels as well as downstream VHL/HIF channels promotes sorafenib resistance. Our findings suggest that the combination of RES-lips with sorafenib reverses changes in PI3K/AKT/mTOR and VHL/HIF signaling pathways. Therefore, we believe that RES-lips could be an alternative combination therapy strategy to overcome sorafenib resistance in RCC patients. In addition, because RES-lips have an anti-sorafenib resistance effect, whether RES-lips can slow the tolerability of existing RCC treatments (such as radiotherapy or chemotherapy) will be a good subsequent research direction. Due to study limitations, deeper exploration of the PI3K-AKT-mTOR and VHL-HIF signaling pathways, validation of these pathways, and toxicology studies of the RES-lips and Sorafenib combination therapy are warranted.

5. Conclusion

In conclusion, the combination of RES-lips with sorafenib achieves synergistic anti-RCC tumor efficacy and can also improve sorafenib resistance in RCC models by modulating PI3K-AKT-mTOR and VHL-HIF signaling pathways. The results of this study provide preclinical data and mechanistic support for the improvement of drug resistance to sorafenib in RCC and enhancing overall anti-RCC efficacy

Funding

Traditional Chinese Medicine Science and Technology Plan Project Zhejiang Province: Based on the combination of sorafenib and polyethylene glycol resveratrol to improve the synergistic therapeutic effect of renal cell carcinoma (2024ZL279). General scientific research project of colleges and universities of Zhejiang Provincial Department of Education: Study on the mechanism of ultrasonic targeted damage technology regulating myocardial fibroblasts in myocardial infarction (Y202352011).

CRediT authorship contribution statement

Ligang Wang: Writing – review & editing, Writing – original draft, Methodology, Investigation, Formal analysis, Data curation, Conceptualization. **Ying Wang:** Writing – review & editing, Writing – original draft, Data curation. **Qiqi Xie:** Writing – review & editing, Writing – original draft, Methodology, Investigation. **Songcheng Xu:** Writing – review & editing, Writing – original draft, Formal analysis, Data curation. **Fei Liu:** Writing – review & editing, Writing – original draft, Software, Resources. **Yang Liu:** Writing – review & editing, Writing – original draft, Software, Resources. **Fuwei Wang:** Writing – review & editing, Writing – original draft, Visualization, Validation. **Weinan Chen:** Writing – review & editing, Writing – original draft, Supervision, Project administration. **Jianchun Li:** Writing – review & editing, Writing – original draft, Supervision, Project administration. **Litao Sun:** Writing – review & editing, Writing – original draft, Supervision, Project administration.

Declaration of competing interest

The authors declare no conflict of interest.

Data availability

Data will be made available on request.

References

Adnane, L., Trail, P.A., Taylor, I., Wilhelm, S.M., 2006. Sorafenib (BAY 43-9006, Nexavar), a dual-action inhibitor that targets RAF/MEK/ERK pathway in tumor cells and tyrosine kinases VEGFR/PDGFR in tumor vasculature. Methods Enzymol. 407, 597–612.

Akkewar, A., Mahajan, N., Kharwade, R., Gangane, P., 2023. Liposomes in the targeted gene therapy of cancer: a critical review. Curr. Drug Deliv. 20, 350–370.

Badoiu, S.C., Greabu, M., Miricescu, D., Stanescu II, S., Ilinca, R., Balan, D.G., Balcangiu-Stroescu, A.E., Mihai, D.A., Vacaroiu, I.A., Stefani, C., Jinga, V., 2023. PI3K/AKT/mTOR dysregulation and reprogramming metabolic pathways in renal cancer: crosstalk with the VHL/HIF axis. Int. J. Mol. Sci. 24.

Bahadoram, S., Davoodi, M., Hassanzadeh, S., Bahadoram, M., Barahman, M., Mafakher, L., 2022. Renal cell carcinoma: an overview of the epidemiology, diagnosis, and treatment. Giornale Ital. Nefrol. 39.

Braun, D.A., Bakouny, Z., Hirsch, L., Flippot, R., Van Allen, E.M., Wu, C.J., Choueiri, T. K., 2021. Beyond conventional immune-checkpoint inhibition - novel immunotherapies for renal cell carcinoma. Nat. Rev. Clin. Oncol. 18, 199–214.

Chang, K., Chen, Y., Zhang, X., Zhang, W., Xu, N., Zeng, B., Wang, Y., Feng, T., Dai, B., Xu, F., Ye, D., Wang, C., 2023. DPP9 stabilizes NRF2 to suppress ferroptosis and induce sorafenib resistance in clear cell renal cell carcinoma. Cancer Res. 83, 3940–3955.

Chen, L., Musa, A.E., 2021. Boosting immune system against cancer by resveratrol. Phytother. Res. 35, 5514–5526.

Choi, C.Y., Lim, S.C., Lee, T.B., Han, S.I., 2022. Molecular basis of resveratrol-induced resensitization of acquired drug-resistant cancer cells. Nutrients 14.

Cui, S.X., Shi, W.N., Song, Z.Y., Wang, S.Q., Yu, X.F., Gao, Z.H., Qu, X.J., 2016. Des-gamma-carboxy prothrombin antagonizes the effects of Sorafenib on human hepatocellular carcinoma through activation of the Raf/MEK/ERK and PI3K/Akt/mTOR signaling pathways. Oncotarget 7, 36767–36782.

Escudier, B., Worden, F., Kudo, M., 2019. Sorafenib: key lessons from over 10 years of experience. Expert. Rev. Anticancer. Ther. 19, 177–189.

Ethemoglu, M.S., Seker, F.B., Akkaya, H., Kilic, E., Aslan, I., Erdogan, C.S., Yilmaz, B., 2017. Anticonvulsant activity of resveratrol-loaded liposomes in vivo. Neuroscience 357, 12–19.

Guimarães, D., Cavaco-Paulo, A., Nogueira, E., 2021. Design of liposomes as drug delivery system for therapeutic applications. Int. J. Pharm. 601, 120571.

He, Y., Luo, Y., Huang, L., Zhang, D., Wang, X., Ji, J., Liang, S., 2021. New frontiers against sorafenib resistance in renal cell carcinoma: from molecular mechanisms to predictive biomarkers. Pharmacol. Res. 170, 105732.

Huang, W.C., Becher, E., 2020. Current landscape of advanced and metastatic renal cell carcinoma management. Urol. Clin. North Am. 47, xiii–xiv.

Jiashuo, W.U., Fangqing, Z., Zhuangzhuang, L.I., Weiyi, J., Yue, S., 2022. Integration strategy of network pharmacology in traditional Chinese medicine: a narrative review. J. Tradit. Chin. 42, 479–486.

Jin, J., Xie, Y., Zhang, J.S., Wang, J.Q., Dai, S.J., He, W.F., Li, S.Y., Ashby Jr., C.R., Chen, Z.S., He, Q., 2023. Sunitinib resistance in renal cell carcinoma: from molecular mechanisms to predictive biomarkers. Drug Resist. Updat. 67, 100929.

Kane, R.C., Farrell, A.T., Saber, H., Tang, S., Williams, G., Jee, J.M., Liang, C., Booth, B., Chidambaram, N., Morse, D., Sridhara, R., Garvey, P., Justice, R., Pazdur, R., 2006. Sorafenib for the treatment of advanced renal cell carcinoma. Clin. Cancer Res. 12, 7271–7278.

Lee, C.C., Huang, P.Y., Hsieh, Y.H., Chen, Y.S., Tsai, J.P., 2022. Melatonin combined with sorafenib synergistically inhibit the invasive ability through targeting metastasis-associated protein 2 expression in human renal cancer cells. Tzu Chi Med. J. 34, 192–199.

Li, Q., Chen, K., Zhang, T., Jiang, D., Chen, L., Jiang, J., Zhang, C., Li, S., 2023. Understanding sorafenib-induced ferroptosis and resistance mechanisms: implications for cancer therapy. Eur. J. Pharmacol. 955, 175913.

Makhov, P., Joshi, S., Ghatalia, P., Kutikov, A., Uzzo, R.G., Kolenko, V.M., 2018. Resistance to systemic therapies in clear cell renal cell carcinoma: mechanisms and management strategies. Mol. Cancer Ther. 17, 1355–1364.

Massari, F., Ciccarese, C., Santoni, M., Brunelli, M., Piva, F., Modena, A., Bimbatti, D., Fantinel, E., Santini, D., Cheng, L., Cascinu, S., Montironi, R., Tortora, G., 2015. Metabolic alterations in renal cell carcinoma. Cancer Treat. Rev. 41, 767–776.

Mei, J., Zhu, X., Wang, Z., Wang, Z., 2014. VEGFR, RET, and RAF/MEK/ERK pathway take part in the inhibition of osteosarcoma MG63 cells with sorafenib treatment. Cell Biochem. Biophys. 69, 151–156.
Miricescu, D., Balan, D.G., Tulin, A., Stiru, O., Vacaroiu, I.A., Mihai, D.A., Popa, C.C., Papacocea, R.I., Enyedi, M., Sorin, N.A., Vatachki, G., Georgescu, D.E., Nica, A.E., Stefani, C., 2021. PI3K/AKT/mTOR signalling pathway involvement in renal cell carcinoma pathogenesis (Review). Exp. Ther. Med. 21, 540.
Msaouel, P., Genovese, G., Tannir, N.M., 2023. Renal cell carcinoma of variant histology: biology and therapies. Hematol. Oncol. Clin. North Am. 37, 977–992.
Oya, M., Kaneko, S., Imai, T., Tsujino, T., Sunaya, T., Okayama, Y., 2022. Effectiveness and safety of sorafenib for renal cell, hepatocellular and thyroid carcinoma: pooled analysis in patients with renal impairment. Cancer Chemother. Pharmacol. 89, 761–772.
Rasmussen, N., Rathmell, W.K., 2011. Looking beyond inhibition of VEGF/mTOR: emerging targets for renal cell carcinoma drug development. Curr. Clin. Pharmacol. 6, 199–206.
Ren, B., Kwah, M.X., Liu, C., Ma, Z., Shanmugam, M.K., Ding, L., Xiang, X., Ho, P.C., Wang, L., Ong, P.S., Goh, B.C., 2021. Resveratrol for cancer therapy: challenges and future perspectives. Cancer Lett. 515, 63–72.
Santoni, M., Pantano, F., Amantini, C., Nabissi, M., Conti, A., Burattini, L., Zoccoli, A., Berardi, R., Santoni, G., Tonini, G., Santini, D., Cascinu, S., 2014. Emerging strategies to overcome the resistance to current mTOR inhibitors in renal cell carcinoma. Biochim. Biophys. Acta 1845, 221–231.
Shi, Y.H., Ding, Z.B., Zhou, J., Hui, B., Shi, G.M., Ke, A.W., Wang, X.Y., Dai, Z., Peng, Y. F., Gu, C.Y., 2011. Targeting autophagy enhances sorafenib lethality for hepatocellular carcinoma via ER stress-related apoptosis. Autophagy 7, 1159–1172.
Sun, H., Zheng, J., Xiao, J., Yue, J., Shi, Z., Xuan, Z., Chen, C., Zhao, Y., Tang, W., Ye, S., Li, J., Deng, Q., Zhang, L., Zhu, F., Shao, C., 2022. TOPK/PBK is phosphorylated by ERK2 at serine 32, promotes tumorigenesis and is involved in sorafenib resistance in RCC. Cell Death Dis. 13, 450.
Tian, B., Liu, J., 2020. Resveratrol: a review of plant sources, synthesis, stability, modification and food application. J. Sci. Food Agric. 100, 1392–1404.
Tian, X., Zhang, S., Zhang, Q., Kang, L., Ma, C., Feng, L., Li, S., Li, J., Yang, L., Liu, J., Qi, Z., Shen, Y., 2020. Resveratrol inhibits tumor progression by down-regulation of NLRP3 in renal cell carcinoma. J. Nutr. Biochem. 85, 108489.
Wang, L., Wu, H., Wang, Y., Xu, S., Yang, C., Zhang, T., Liu, Y., Wang, F., Chen, W., Li, J., Sun, L., 2023. Synergistic anti-tumour activity of sorafenib in combination with pegylated resveratrol is mediated by Akt/mTOR/p70S6k-4EBP-1 and c-Raf7MEK/ERK signaling pathways. Heliyon 9, e19154.
Yang, L., Shi, L., Fu, Q., Xiong, H., Zhang, M., Yu, S., 2012. Efficacy and safety of sorafenib in advanced renal cell carcinoma patients: results from a long-term study. Oncol. Lett. 3, 935–939.
Zhang, H., Zhu, G., 2021. Predictive biomarkers and novel targets in the treatment of metastatic renal cell carcinoma. Curr. Med. Chem. 28, 5213–5227.
Zhu, X.W., Dong, F.M., Liu, J., Li, M.S., 2022. Resveratrol nanoparticles suppresses migration and invasion of renal cell carcinoma cells by inhibiting matrix metalloproteinase 2 expression and extracellular signal-regulated kinase pathway. J. Biomed. Nanotechnol. 18, 1001–1008.
Zupančič, Š., Lavrič, Z., Kristl, J., 2015. Stability and solubility of trans-resveratrol are strongly influenced by pH and temperature. Eur. J. Pharm. Biopharm. 93, 196–204.